Numerical Methods in Civil Engineering, 10-4 (2026) 108-119



Numerical Methods in Civil Engineering

Journal Homepage: https://nmce.kntu.ac.ir/

Comparative Thermal Behaviour of Unprotected and Protected Steel, Stainless Steel, and Aluminium Framed Buildings Exposed to Standard Fire

Kuldeep Joshi [*], **Archana Bohra Gupta** [**]

ARTICLE INFO

RESEARCH PAPER

Article history:
Received:
June 2026
Revised:
October 2026
Accepted:
November 2026

Keywords:
Thermal analysis; Different metallic materials; Standard fire; Finite element method; Magnesium oxide board

Abstract:

Fire significantly influences the thermal and structural behaviour of metallic-framed buildings by reducing strength and stability at elevated temperatures. This study presents a comparative thermo-mechanical assessment of steel, stainless steel, and aluminium-framed buildings subjected to fire. For the comparative analysis, we modelled a three-storey (G+2) building and analysed it under a 30-minute standard fire exposure using the finite element software Abaqus. The G+2 building comprises a ground floor plus two upper stories. The results show that, due to fire, the building experiences increased stress and plastic strain accumulation regardless of the type of metal (Steel, Stainless steel, or Aluminium) used in its construction. We also evaluated the critical temperature, which was lowest for the stainless steel frame and highest for the aluminium frame, while the steel frame exhibited intermediate behaviour. Further reaction force analysis indicated that stainless steel retained the highest load-carrying capacity during fire, steel showed moderate performance, while aluminium experienced the fastest degradation in structural strength. In addition, we studied the role of a passive fire protection layer in mitigating the fire-induced instability. We evaluated different thicknesses of magnesium oxide board (1-15 cm) under a 30-minute standard fire temperature and found that it reduced the temperature by 11.14% to 95.41%, respectively. The minimum required thickness of magnesium oxide board to preserve the building's structural integrity for 30 minutes was also determined based on the critical temperature. It was found to lie in the range of 8-11 cm for different metals considered in this study.

1. Introduction

Fire represents one of the most severe accidental loading conditions that can affect the safety and stability of building structures. Elevated temperature during fire exposure significantly alters the thermal and mechanical properties of structural materials, resulting in degradation of stiffness, reduction in strength, thermal expansion, and eventually structural instability or collapse [1-2]. In modern urban and industrial environments, framed structures constructed using steel and lightweight metallic materials are increasingly adopted because of their high strength-to-weight ratio and rapid construction [3-4].

* *Corresponding author: Ph.D. Candidate, Department of Structural Engineering, MBM University, Jodhpur, India. Email: kuldeepj.phdse@mbm.ac.in*
** *Professor, Department of Structural Engineering, MBM University, Jodhpur, India.*

However, these materials are highly sensitive to elevated temperatures, making fire safety assessment an essential design step [5]. Among metallic construction materials, although steel is widely used, in recent years stainless steel and aluminium alloys have emerged as alternative framing materials because of their superior corrosion resistance, durability, and lightweight characteristics [6-7]. However, these materials possess different thermal and mechanical properties compared to structural steel, which can considerably influence the thermal and structural response of framed buildings in fire. Therefore, a comparative assessment of steel, stainless steel, and aluminium framed buildings under fire is essential for understanding their thermo-mechanical behaviour and ensuring safety and economical structural design.

https://doi.org/10.66224/NMCE.2606.1149

Past research has thoroughly examined how structural steel components react during fire exposures. For example, when steel beams are subjected to fire, they mainly fail due to a mix of local buckling and lateral or longitudinal buckling, and the significant interaction between these modes results in a notable decrease in their load-bearing capacity [8]. Ibraheem and Abdllah [9] noted that at higher temperatures, the beam may lose over 50% of its flexural strength and 38% of its shear strength, in comparison to conditions at ambient temperatures. Such thermal degradation also changes the buckling behaviour of steel beams, leading their capacity to diverge from existing design guidelines. A similar pattern was observed in steel columns, where failure primarily resulted from buckling due to fire, yet the extent of this failure is significantly affected by the axial and rotational constraints provided by the support [10-13]. In terms of fire protection strategies, Anvari et al. [14] have illustrated the advantage of encasing steel components in concrete, particularly in the oil sector, while Aghabozorgi et al. [15] have highlighted the effectiveness of gypsum mortars in slowing the temperature increase in steel columns.

Most previous fire engineering studies have focused on conventional structural steel, while comparatively little research has been conducted on stainless steel and aluminium-framed buildings under elevated temperatures. Existing investigations generally evaluate these materials independently, and direct comparative assessment under identical geometry, loading, and fire conditions remains limited. Furthermore, a large portion of studies is limited to isolated structural members, such as beams, columns, and joints, rather than to the global thermo-mechanical behaviour of complete framed buildings. Moreover, the suitability of a passive fire protection layer for different metallic framing systems has not been comprehensively investigated. Limited research has also been conducted on determining the minimum required fire protection thickness necessary to preserve the structural integrity of steel, stainless steel, and aluminium framed buildings under fire conditions.

Most previous fire resistance studies have been conducted at component levels. This current study provides an overview of the thermo-mechanical behaviour of full-scale steel, stainless steel, and aluminium framed buildings. The same frame geometry, loading conditions, and fire exposure (30-min standard fire) were applied to all three structural systems using a common finite element model. This allows comparisons between stress development, plastic strain, displacement, critical temperature, and reaction forces in each material. In addition to studying unprotected frames, the effect of magnesium oxide board as a passive fire protection material is investigated. This enables the minimum thickness of passive fire protection to be determined for each frame type based on the critical temperature criteria. A greater overview of the fire performance of these metallic structural systems can therefore be gained. The main contribution of this study is that the whole frame can be assessed, as well as the protection requirements for each material.

2. Methodology

To comparatively study the fire response of a steel, stainless steel, and aluminium framed building, a three-dimensional deformable solid finite element model of a three-storey (G+2) building is modelled and analysed through finite element software Abaqus, as shown in Fig.1. The geometric properties of the building and characteristics of structural members are represented in Table 1. The frame is assigned temperature-dependent properties of steel, stainless steel, and aluminium sequentially to undertake the comparative study. For the analysis, the coupled temperature-displacement (Transient) approach of Abaqus was employed, using an 8-node thermally coupled brick, trilinear displacement and temperature elements (C3D8T). This study comprises two parts:

1. Comparative analysis of the building under the same geometric, loading, and support conditions but with different metallic materials (Steel, Stainless Steel, and aluminium) under a 30-minute standard fire.
2. Analysing different thicknesses of magnesium oxide board for their temperature-reducing capabilities and finding their minimum required thickness to preserve the structural integrity of the building under different metallic material configurations.

Table 1: Geometric properties of the building and characteristics of structural members

Geometric Configuration of Building		**Member Dimension**	
No of Storeys	3	Beam (I-Section Configuring to ISMB 300)	Depth: 300 mm Width of Flange: 140 mm Thickness of Flange: 12.4 mm Thickness of Web: 7.5 mm
No of Bays (In X and Z Directions Each)	2	Column (I-Section Configuring to ISHB 300)	Depth: 300 mm Width of Flange: 250 mm Thickness of Flange: 10.6 mm Thickness of Web: 7.6 mm
Size of Each Bay	5 m * 5 m		
Length of Beam	5 m		
Height of Each Storey	3 m		

Here,
ISMB and ISHB refer to Indian Standard Medium Weight Beam and Indian Standard Heavy Weight Beam, respectively, having configurations as per SP 6(1): 1964 (Reaffirmed 2003) [16]

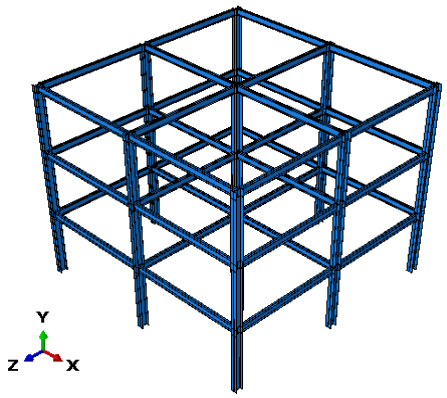


Fig. 1: Three-dimensional model of a building

2.1. Material Properties

The building frame materials (Steel, Stainless steel, or Aluminium) were assumed to have a yield strength of 250 N/mm^2. Accordingly, E-250 grade steel, austenitic-based stainless steel (Grade 304), and 6061-T6 aluminium were considered. The mechanical properties of these grades at ambient temperature (20°C) are presented in Table 2, while the temperature-dependent variation of their thermal and mechanical properties is presented in Tables 3, 4, and 5, respectively, as per EN 1993-1-2 [17] and EN 1999-1-2 [18]. A comparative variation of the mechanical and thermal properties of steel, stainless steel, and aluminium with temperature is shown in Fig. 2 and Fig. 3.

Table 2: Properties of structural steel, stainless steel, and aluminium at ambient temperature

	Density (Kg/m^3)	Poisson's Ratio	Modulus of Elasticity (N/m^2)	Yield Strength (N/m^2)
Steel	7850	0.3	2E+11	250000000
Stainless Steel	7850	0.3	2E+11	250000000
Aluminium	2700	0.33	7E+10	250000000

Table 3: Temperature-dependent variation of thermal and mechanical properties of steel

Temperature (°C)	Specific Heat (J/KgK)	Thermal Conductivity (W/mK)	Coefficient of Thermal Expansion (/°C)	Yield Strength (N/m^2)	Modulus of Elasticity (N/m^2)
20	439.80176	53.3	0.00001216	250000000	2E+11
100	487.62	50.7	0.0000128	250000000	2E+11
200	529.76	47.3	0.0000136	250000000	1.80E+11
300	564.74	44	0.0000144	250000000	1.60E+11
400	605.88	40.7	0.0000152	250000000	1.40E+11
500	666.5	37.4	0.000016	195000000	1.20E+11
600	760.2173913	34	0.0000168	117500000	6.20E+10
700	1008.157895	30.7	0.0000176	57500000	2.60E+10
800	803.2608696	27.3	0	27500000	1.80E+10
900	650	27.3	0.00002	15000000	1.35E+10
1000	650	27.3	0.00002	10000000	9.00E+09
1100	650	27.3	0.00002	5000000	4.50E+09
1200	650	27.3	0.00002	1	1

Table 4: Temperature-dependent variation of thermal and mechanical properties of stainless steel

Temperature (°C)	Specific Heat (J/KgK)	Thermal Conductivity (W/mK)	Coefficient of Thermal Expansion (/°C)	Yield Strength (N/m^2)	Modulus of Elasticity (N/m^2)
20	455.5171	14.854	0.00001654	250000000	2E+11
100	476.034	15.87	0.00001711	215000000	1.92E+11
200	498.672	17.14	0.00001783	180000000	1.84E+11
300	518.718	18.41	0.00001854	167500000	1.76E+11
400	536.976	19.68	0.00001926	155000000	1.68E+11
500	554.25	20.95	0.00001998	150000000	1.6E+11
600	571.344	22.22	0.00002069	140000000	1.52E+11
700	589.062	23.49	0.00002141	125000000	1.42E+11
800	608.208	24.76	0.00002212	102500000	1.26E+11
900	629.586	26.03	0.00002284	55000000	9E+10
1000	654	27.3	0.00002356	35000000	4E+10
1100	682.254	28.57	0.00002427	17500000	2E+10

Table 5: Temperature-dependent variation of thermal and mechanical properties of aluminium

Temperature (°C)	Specific Heat (J/KgK)	Thermal Conductivity (W/mK)	Coefficient of Thermal Expansion (/°C)	Yield Strength (N/m^2)	Modulus of Elasticity (N/m^2)
20	911.2	191.4	2.29E-5	250000000	7E+10
50	923.5	193.5	2.35E-5	-	693E+8
100	944	197	2.45E-5	250000000	679E+8
150	964.5	200.5	2.45E-5	245000000	651E+8
200	985	204	2.45E-5	142500000	602E+8
250	1005.5	207.5	2.45E-5	77500000	546E+8
300	1026	211	2.45E-5	47500000	476E+8
350	1046.5	214.5	2.45E-5	32500000	378E+8
400	1067	218	2.45E-5	-	28E+9
450	1087.5	221.5	2.45E-5	-	-
500	1108	225	2.45E-5	-	-
550	-	-	-	1	1

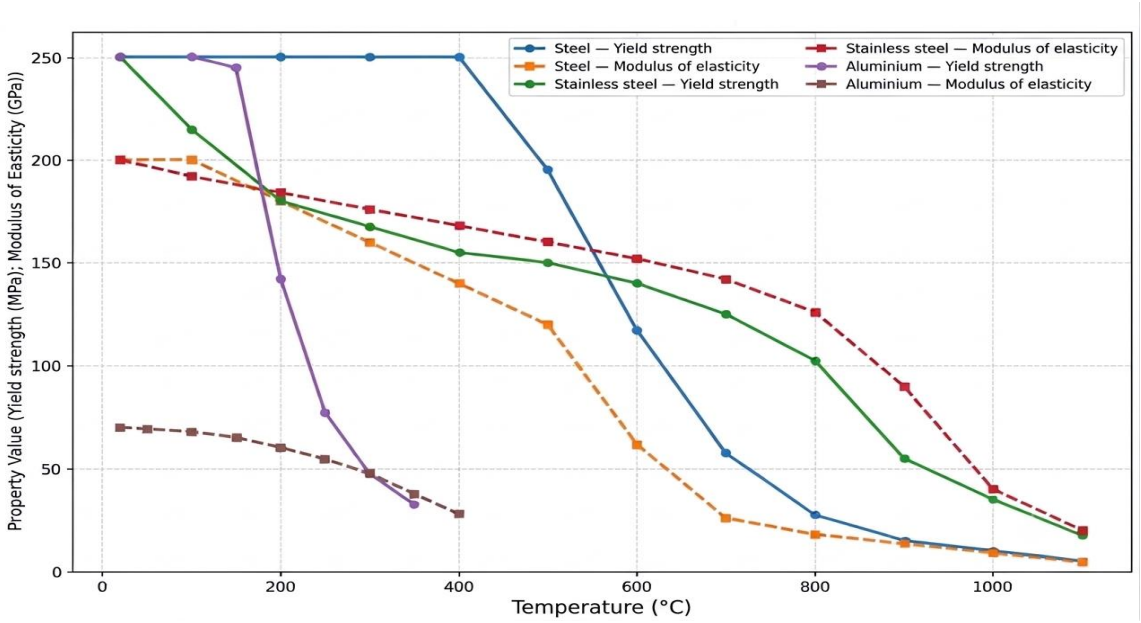


Fig. 2: Comparative variation of mechanical properties of steel, stainless steel and aluminium with temperature

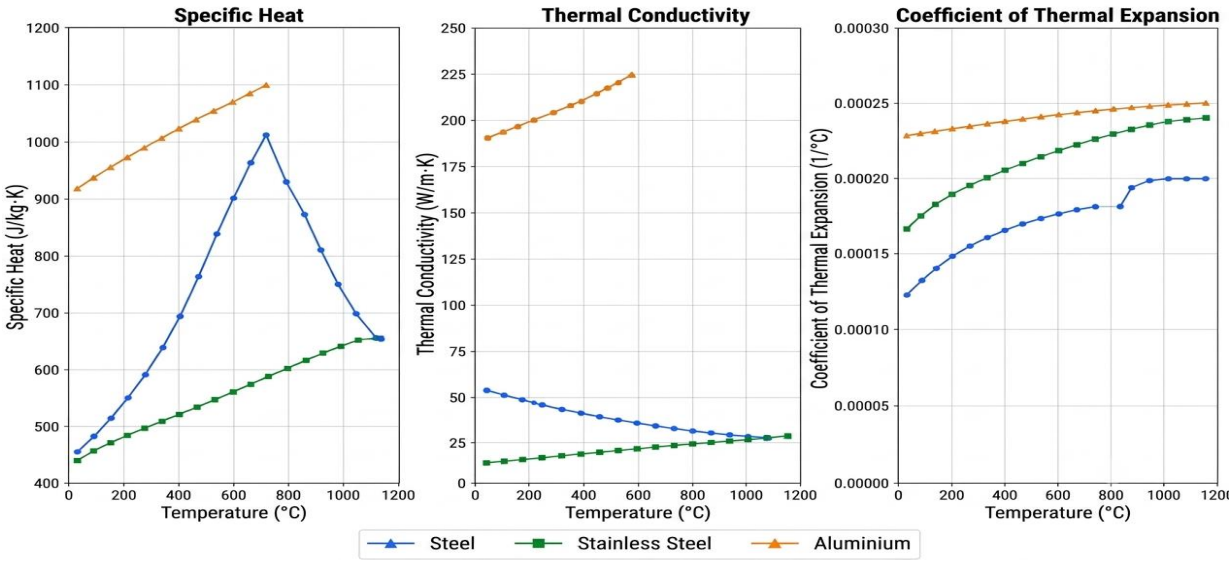


Fig. 3: Comparative variation of thermal properties of steel, stainless steel and aluminium with temperature

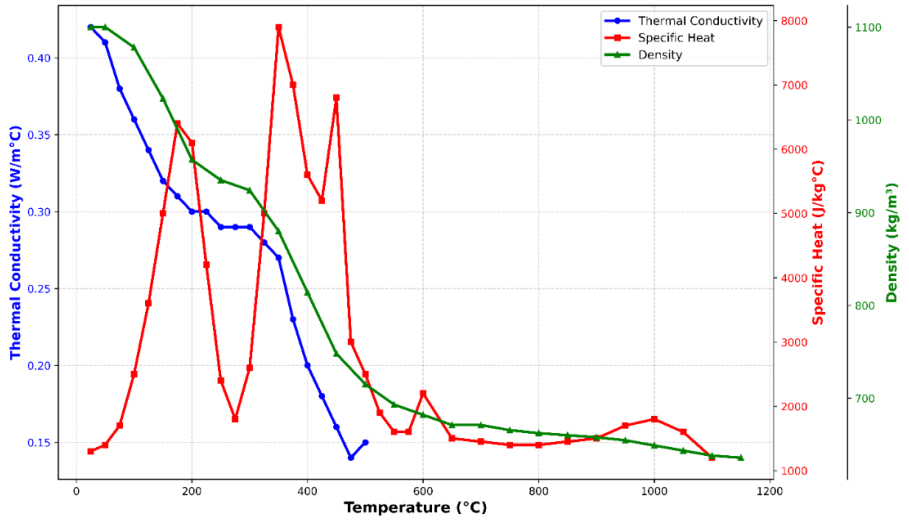


Fig. 4: Variation of thermal properties of magnesium oxide board with

2.2 Fire Protection Layer

In this study, we considered magnesium oxide board as a fire protective layer. We considered various board thicknesses (1-15 cm) and evaluated their temperature-reducing capability using the temperature-time variation curve. The temperature-dependent variation of the thermal properties of magnesium oxide board has been taken in accordance with [19], as shown in Fig. 4. Magnesium oxide board is only considered as a fire protection coating; its mechanical properties have been neglected.

2.3. Support Condition and Beam Column Connection

The base of the ground-storey columns were modeled as fixed supports, restraining all translational and rotational degrees of freedom. The beam-column connection was considered rigid, using a tie constraint between the column and beam without explicitly modelling a detailed connection, because this study aims to compare the fire response of steel, stainless steel, and aluminium framed buildings rather than studying the behaviour of the joint. However, joint type can affect the building's fire response, but this forms a separate study. Therefore, joint simplification is considered a limitation of the current study.

2.4. Loading

The following loads are considered to act on the building:

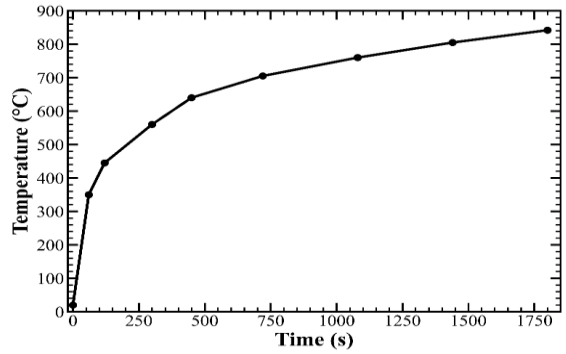
1. Self-Weight: The self-weight of the structure is introduced through gravity loading using the acceleration due to gravity as 9.81 m/s^2.
2. Self-Weight of Concrete Slab, Finishing Load, and Imposed Load
   a. A cement concrete slab of 150 mm thickness was assumed to be acting as a floor in the building. The self-weight of the slab was calculated by multiplying the concrete unit weight (25 KN/m^3) by the slab thickness, giving it as 3.75 KN/m^2.
   b. The finishing load was assumed to be equal to 1 KN/m^2.
   c. The building was assumed to have an industrial occupation, with light-duty machinery/equipment. Accordingly, an imposed load of 5 KN/m^2 was taken to act on the cement concrete slab, as per IS 875 (Part 2): 1987 (Reaffirmed 2003) [20].

   All the above loads (a-c) were applied on the beams as pressure (As per their tributary widths). For the edge beam, the tributary width is 1.25 m, and the applied pressure is 87.1 KN/m^2. For the interior beam, the tributary width is 2.5 m, and the applied pressure is 174.3 KN/m^2

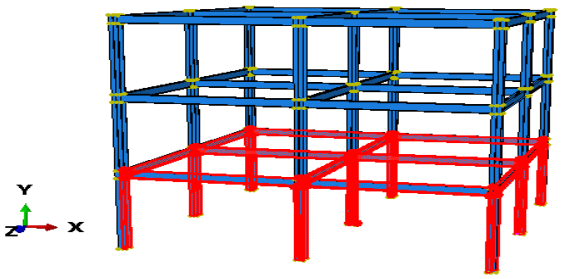
2.5. Fire Profile, Thermal Boundary Condition, and Analysis Cases

The fire profile was taken to match the 30-minute (An ideal time in which fire is typically suppressed by firefighting departments) temperature time variation of standard fire (Fig. 5 (a)) as given by EN 1991-1-2 [21]. The fire was assumed to be inside the building; therefore, only the interior portions of all ground-storey beams and columns are heated, as shown in Fig. 5 (b) (Highlighted in red). The fire is directly applied to the surface of the structural elements. The following cases are considered in this study:

Case 1: Steel-framed building subjected to standard fire
Case 2: Stainless steel-framed building subjected to standard fire
Case 3: Aluminium-framed building subjected to standard fire



(a)



(b)

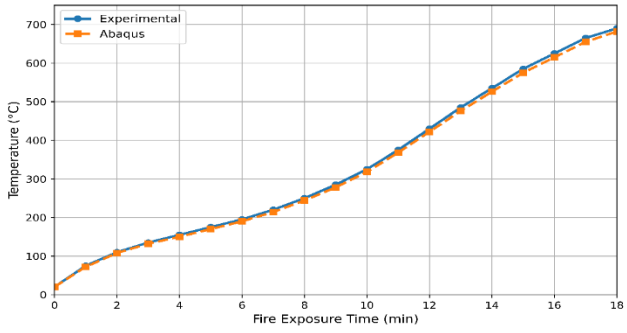
Fig. 5: (a) Temperature-time variation of standard fire, **(b)** Thermal boundary condition of building

For clarity and reproducibility, the thermal boundary conditions adopted in the finite element model are summarised here. The ambient temperature is taken as 20°C. The convective heat transfer coefficient on the fire-exposed surface is 25 W/m²K, in accordance with Eurocode recommendations for standard fire exposure. The convective heat transfer coefficient on the unexposed surfaces is 10 W/m²K. The surface emissivities of steel, stainless steel, and aluminium are 0.70, 0.4, and 0.3, respectively. Radiation heat transfer was modelled using the Stefan–Boltzmann law with a radiation constant of 5.67×10^{-8} W/m²K⁴. The fire-exposed surface was subjected simultaneously to convection and radiation, with the gas temperature defined by the Eurocode 1 standard fire curve. The unexposed surfaces exchanged heat with the surrounding environment by convection and radiation at an ambient temperature of 20 °C.

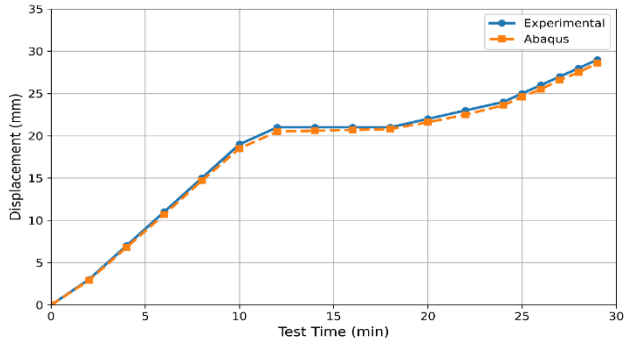
2.6. Model Validation and Mesh Sensitivity Analysis

The modelling approach used in this study employed a fully coupled temperature-displacement formulation with temperature-dependent material properties specified in EN 1993-1-2 [17] and EN 1999-1-2 [18]. EN 1991-1-2 [21] defines the fire curves based on extensive experimental calibration. The modelling approach follows established thermo-mechanical finite element procedures, commonly used in validated structural fire research. The framework captures key fire-induced mechanisms, including restrained thermal expansion, thermal bowing, stiffness degradation at elevated temperatures, and residual stress development after cooling, as reported in previous studies involving fire evaluation of steel subjected to fire [22-24]. To further

validate the finite element model, the experimental study by Ramesh et al. [25] on steel beams subjected to localised fire exposure was numerically replicated in Abaqus. The beam had a total length of 6.2 m with a simply supported span of 5.87 m, fabricated using ASTM A992 steel. The experimental program involved W16x26 steel beams exposed to localised fire beneath the beam mid-span. The beam was loaded by two point loads of 90 kN each, before fire exposure. To replicate the experiment in Abaqus, the same boundary conditions and a coupled temperature-displacement approach with a 10 mm mesh size and C3D8T elements were used. Figures 6 (a) and (b) show the variation of temperature attained by the beam bottom flange and mid-span deflection with time obtained in the experiment and numerical simulation in Abaqus. A close agreement in temperature development and deflection was observed between the experimental and simulation data, thus validating the capability of the finite element methodology in capturing fire-induced changes in structural response. Another experimental study by Rubert and Schaumann [26] was also replicated in Abaqus using a coupled temperature-displacement approach with a 10 mm mesh size and C3D8T elements. The experimental work comprises uniformly heating a simply supported steel beam (Made of an IPE 80 section) along its full length. The beam section was loaded with a central point load having a magnitude equal to 0.7 times the bending capacity of the beam. Figures 7 (a) and (b) show the variation of temperature attained by the bottom flange of the beam with time and mid-span displacement of the beam versus temperature, respectively, obtained in the experiment and numerical simulation in Abaqus. The close agreement between experimental and Abaqus results further validates the modelling approach used in this study.

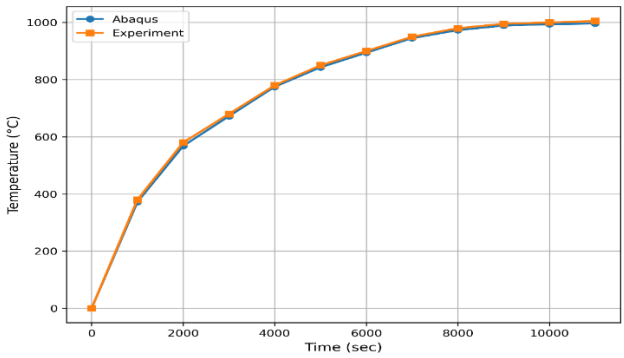


(a)

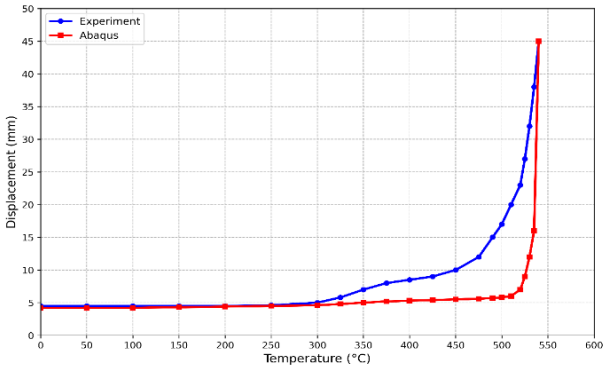


(b)

Fig. 6: (a) and **(b)**: Experimental validation of the finite element model according to study by Ramesh et al. [25]



(a)



(b)

Fig. 7: (a) and **(b)**: Experimental validation of the finite element model according to the study by Rubert and Schaumann [26]

To ensure that the current study results are free from mesh size effects, a mesh sensitivity analysis was performed on Case 1 (of this study) using global mesh sizes of 25 mm, 20 mm, and 15 mm. The post-fire Von Mises stress and plastic strain values in the building were evaluated for each mesh size. For a 25 mm mesh size, the stress and strain values obtained were 457.6 MPa and 0.094, respectively. For a 20 mm mesh size, they were 440 MPa and 0.09, respectively, and for a 15 mm mesh size, they were 431.2 MPa and 0.087, respectively. The difference in stress and strain values obtained for 25 mm and 20 mm meshes was 4 to 5%, while the difference between the values obtained with 20 mm and 15 mm meshes was 2 to 3%, indicating that the solution converged with mesh refinement. Therefore, we adopted the 20 mm mesh to balance accuracy and computational cost.

As the current study also involves an aluminium-framed building, a mesh sensitivity analysis is also performed for (Case 3) using the same global mesh sizes of 25 mm, 20 mm, and 15 mm. For a 25 mm mesh size, the stress and strain values obtained were 277.83 MPa and 0.064, respectively. For a 20 mm mesh size, they were 264.6 MPa and 0.062, respectively, and for a 15 mm mesh size, they were 256.6 MPa and 0.059, respectively. The difference in stress and strain values obtained for 25 mm and 20 mm meshes was 5 to 7%, while the difference between the values obtained with 20 mm and 15 mm meshes was 3 to 4%, indicating that the solution converged with mesh refinement. Based on these mesh sensitivity studies, a 20 mm mesh size was adopted to balance accuracy and computational cost.

3. Results and Discussions

3.1. Results

The thermal and structural parameters, viz., the maximum temperature attained by the structure, the stress (Von Mises), the plastic strain (PEEQMAX), and the structural displacements, were determined at the end of the fire under both unprotected and protected conditions. The critical temperature was evaluated for the building frame and subsequently used to find the minimum thickness of magnesium oxide board required to preserve the integrity of the frame in fire. The nomenclature used in the subsequent sections is mentioned at the end of the paper. 3.1.1 Thermal and Structural Parameters Under Unprotected Condition

Table 6 presents the thermal and structural parameters obtained at ambient temperature (20°C) and at the end of the fire, together with their permissible values**.** The following trends are observed:

1. Temperature
   In all cases, the maximum temperature attained by the building frame is equal to the peak magnitude of the standard fire at 30 minutes, i.e., 841.8°C.
2. Stress and Strain in Steel
   For Case 1, the stress magnitude in steel shows a rise from 187.8 MPa to 440 MPa, while the plastic strain increases from 0 to 0.096. For Case 2, the stress magnitude in stainless steel shows a rise from 187.8 MPa to 261.7 MPa, while the plastic strain increases from 0 to 0.088. For Case 3, the stress magnitude in aluminium shows a rise from 182.4 MPa to 264.6 MPa, while the plastic strain increases from 0 to 0.062.
   Thus, in all the cases considered, the stress in different metallic materials exceeds the yield strength of 250 MPa, while plastic strain appears in the structure.
3. Structural Displacement
   a) Beam Deflection (U_2)
      The mid-span deflection of the beam is measured, and across all cases, a decrease in beam deflection was observed. Under Case 1, it decreases from 0.005 m to 0.000005 m; in Case 2, it decreases from 0.005 m to 0.003 m; and in Case 3, it decreases from 0.016 m to 0.00032 m.
   b) Lateral Displacement of Building (U_1 and U_3)
      The lateral displacement of the building was measured at the top of the ground storey column. For Case 1, U_1 increases from 0.0001 m to 0.0003 m, while U_3 decreases from 0.0001 m to 0.00008 m. For Case 2, U_1 increases from 0.0001 m to 0.0002 m, while U_3 decreases from 0.0001 m to 0.00009 m. For Case 3, it is reversed. Here, U_1 decreases from 0.0003 m to 0.0002 m, while U_3 increases from 0.0003 m to 0.0004 m.

The lateral displacements in the building and beam deflection do not exceed the permissible values of 0.006 m and 0.016 m, respectively, as per IS 800:2007 [27].

Table 6: Thermal and structural parameters of the building under unprotected condition

Parameter	Case 1		Case 2		Case 3		Permissible Value
	Ambient Temperature	Fire	Ambient Temperature	Fire	Ambient Temperature	Fire	
Temperature (°C)	20	841.8	20	84.8	20	84.8	-
S, Mises (MPa)	187.8	440	187.8	261.7	182.4	264.6	250 MPa
PEEQMAX	0	0.096	0	0.088	0	0.062	-
Beam Deflection							
U_2 (m)	0.005	0.000005	0.005	0.0003	0.016	0.00032	0.016 m (Span of beam/300)
Lateral Displacement of Building							
U_1 (m)	0.0001	0.0003	0.0001	0.0002	0.0003	0.0002	0.006 m (Height of column/500)
U_3 (m)	0.0001	0.00008	0.0001	0.00009	0.0003	0.0004	

3.1.1 Critical Temperature

Table 6 shows that only the stress values exceed the yield point, while plastic strain begins to develop. In addition, the beam displacement and the building's lateral displacements remain within their permissible limits. Therefore, only stress and strain parameters were considered for the critical temperature evaluation. Based on stress, the critical temperature is considered as the temperature at which stress in steel exceeds the yield stress (250 MPa), while on the basis of strain, the temperature at which the plastic strain starts accumulating is considered as a critical temperature, as presented in Table 7. The critical temperature values obtained based on stress and plastic strain criteria were found to be the same. The maximum critical temperature (85°C) was observed in Case 3, while the least (60°C) was observed in Case 2.

Although temperature-dependent thermal and mechanical properties were incorporated into the finite element models, the critical temperature in this study was determined using **a** fixed ambient-temperature yield strength of 250 MPa. The critical temperature was defined as the local material temperature at the first occurrence of computed stress exceeding this fixed reference value. Thus, the stress-based criterion did not use the temperature-dependent yield

strength as the threshold for determining critical temperature. The critical temperatures reported in Table 7, therefore, represent the results of the specified fixed ambient-yield-strength criterion.

Table 7: Critical temperature under different cases

Parameter	Critical Temperature (°C)		
	Case 1	Case 2	Case 3
S, Mises (MPa)	71	60	85
PEEQMAX	71	60	85

3.1.2 Fire Protection Layer

Fig. 8 shows the temperature-time variation of different thicknesses (1- 15 cm) of magnesium-oxide board under a 30-minute standard fire. It can be noticed that the magnesium oxide board is capable of reducing the peak fire temperature (841.8°C). The highest temperature reduction was achieved using the 15 cm thick board, which reduced the temperature by 95.41%, whereas the lowest reduction of 11.14% was observed with the 1 cm thick board.

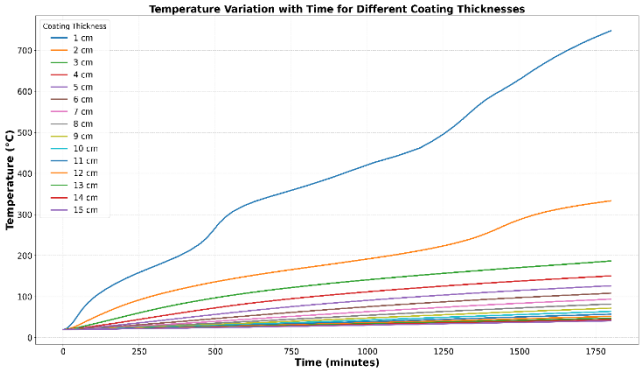


Fig. 8: Temperature time variation of different thicknesses of magnesium oxide board under a 30-minute standard fire

3.1.3 Thermal and Structural Parameters Under Protected Condition

The minimum thickness of magnesium oxide board required to preserve the structural integrity of the building frame under a 30-minute fire was determined based on the critical temperature as described in Section 3.1.2. Using Table 7 and Fig. 6, the board thickness capable of maintaining the temperature of the structure below the critical temperature was determined. Based on this, in Case 1, the required board thickness comes out to be 10 cm; in Case 2, it comes to 11 cm, and in Case 3, it comes out to 8 cm. Table 8 presents the thermal and structural parameters of the building with the above-described magnesium oxide board thicknesses. They show that the steel stress remains below the yield stress (250 N/mm^2), while the plastic strain disappears.

Table 8: Thermal and structural parameters of the building under protected condition

Parameter	Case 1	Case 2	Case 3
Temperature (°C)	64.19	57	82.15
S, Mises (MPa)	192	215	187
Plastic Strain	0	0	0

3.2 Discussions

3.2.1 Unprotected Condition

Fig. 9 (a) and (b) present the comparison of Von Mises stress and plastic strain (PEEQMAX) obtained for cases 1-3 (Steel, stainless steel, and aluminium-framed building) under ambient temperature and fire conditions. A significant increase in stress and accumulation of plastic strain can be observed in all metallic materials after exposure to the 30-minute standard fire. This behaviour mainly occurs because elevated temperature causes thermal expansion of structural members while simultaneously reducing their stiffness and strength, aligning with the findings of Xing et al. [28]. Due to the restraint to thermal expansion offered by the support, beam-column joints, and cooler portions of the structure, additional thermal stresses develop within the structure, leading to yielding and plastic deformation [29-30]. Under ambient temperature, in all cases the frame exhibits lower stress values, namely 187.44 MPa for steel, 187.4 for stainless steel, and 182.4 MPa for aluminium, which are below the yield strength of 250 MPa. No plastic strain is observed under ambient conditions, indicating purely elastic behaviour of the structure. However, after fire exposure, the stress values increase considerably and exceed the yield strength in all cases, initiating plastic strain. Among all the cases, the steel frame (Case 1) develops the highest stress under fire, reaching 440 MPa, together with the maximum plastic strain of 0.096. This behaviour is attributed to the rapid degradation of the elastic modulus and yield strength of structural steel at elevated temperatures. Steel also possesses high thermal conductivity, allowing the heat to spread quickly throughout the section, producing a more uniform temperature rise and longer restrained thermal expansion. Because the structure attempts to expand against restraint, thermal stress develops, and extensive yielding and plastic deformation ultimately occur, similar to that advocated by Allam et al. [31] and Wang et al. [32]. In contrast, the stainless steel frame (Case 2) shows comparatively lower stress and strain values under fire, with stress reaching 261.7 MPa and plastic strain reaching 0.088. Stainless steel exhibits superior thermal performance because it retains a larger proportion of its mechanical strength and stiffness at elevated temperatures compared with steel [17]. Moreover, the lower thermal conductivity of stainless steel reduces the rate of heat transfer through the structural members, thereby delaying temperature penetration and moderating thermal stress development. Owing to this characteristic, stainless steel demonstrates improved resistance against fire-induced degradation and lower plastic deformation, a trend similar to what was observed by Lopes et al. [33]. The aluminium frame (Case 3) develops a fire-induced stress of 264.6 MPa and a plastic strain of 0.062, compared to what was observed in steel and stainless steel cases. Although aluminium possesses very high thermal conductivity, its relatively low modulus of elasticity permits greater thermal deformation and stress redistribution within the structure. This reduces the magnitude of restrained thermal stress generated during fire exposure. Additionally, the lower self-weight of aluminium members reduces gravity-induced stress in the structure. Consequently, despite significant thermal exposure, the

aluminium frame exhibits the least plastic strain accumulation among all cases. Such a trend in the case of the aluminium frame closely aligns with the findings of Maljaars et al. [34] and Milan et al. [35].

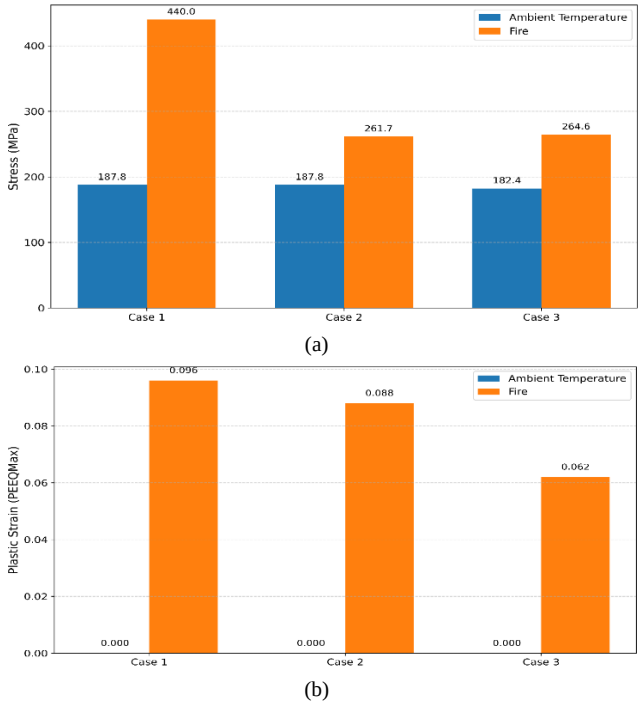


Fig. 9: Comparison of **(a)** stress and **(b)** strain in the building frame in ambient and fire conditions under different cases

3.2.2 Failure Analysis

The comparative analysis reveals distinct thermal-mechanical behaviour for steel, stainless steel and aluminium frames under fire, with critical temperatures of 71°C, 60°C, and 85°C, respectively. The stainless steel frame (Case 2) exhibits the lowest critical temperature. This is mainly because of its lowest thermal conductivity among the three metallic materials considered [17], which slows heat transfer and creates stress concentrations. Apart from this, the degradation in yield strength of stainless steel is also at a fast rate, thus making stress in steel quickly exceed yield strength, explaining why stainless steel shows the lowest critical temperature, similar to what was observed by Zanoni et al. [36] and Chen et al. [37] in their studies. For the steel frame (Case 1), the critical temperature is intermediate. Steel has relatively high thermal conductivity, which allows heat to spread uniformly across the section. This uniform heating produces significant restrained thermal expansion and stress buildup. At the same time, steel's modulus of elasticity and yield strength degrade rapidly with temperature. Compared to stainless steel, steel retains strength slightly longer, delaying yield exceedance, explaining why steel lies in the middle range of critical temperatures, a similar phenomenon previously verified by Choi et al. [38]. The aluminium frame (Case 3) exhibits the highest critical temperature. Although aluminium has very high thermal conductivity, its low modulus of elasticity allows larger thermal deformations and stress redistribution, reducing residual thermal stress concentration. Additionally, aluminium's lower self-weight reduces gravity-induced stresses in the frame; these mechanisms collectively delay the onset of yielding, resulting in the highest critical temperature among the three metallic materials considered, consistent with the findings of Sabtu et al. [39] and Petre [40].

Fig. 10 shows the comparative variation of reaction force (measured at the base of the ground-storey column) with time for Steel (Case 1), Stainless Steel (Case 2), and Aluminium (Case 3) frame building under a 30-minute fire. The figure clearly highlights the influence of different thermal and mechanical properties of metallic materials on the structural response. At the initial heating stage, all three cases exhibit a rapid increase in reaction force. This increase occurs primarily because the heated structure attempts to expand thermally, but is restrained by the cooler portion and support. However, the magnitude of this increase varies significantly among the three metallic materials because of differences in thermal conductivity, modulus degradation, and elevated temperature strength retention [17]. Amongst all cases, the stainless steel frame developed the highest reaction force throughout the fire. The reaction force increases sharply and peaks at 2.8×10^5 N at 120 sec. After the peak, the reaction force decreases gradually and remains nearly 1.25×10^5 N at the end of 1800 sec of fire exposure. Compared with steel and aluminium, stainless steel retains a large proportion of its stiffness and yield strength at elevated temperatures. The steel frame exhibits intermediate behaviour between stainless steel and aluminium. The reaction force increases rapidly during the early stage of fire and peaks at 1.4×10^5 N at nearly 150 sec, almost 50% lower than the peak value observed in stainless steel. Thereafter, the reaction force decreases gradually with time and reaches 0.8×10^5 N at 1800 sec. Compared with stainless steel, the elastic modulus and yield strength of structural steel degrade faster at elevated temperatures. Although steel has relatively high thermal conductivity, allowing heat to spread more uniformly across the section, this also accelerates the frame's overall thermal softening, as verified by Chi et al. [41] and Zayniddinov et al. [42]. Consequently, the frame progressively loses stiffness and undergoes stress redistribution, causing a continuous reduction in support reactions. However, the steel frame remains stable during the entire 30-minute fire without collapse. The aluminium frame (Case 3) demonstrates the most critical behaviour under fire exposure. Initially, the reaction forces rise very sharply and reach 2.1×10^5 N within only 30-40 s, indicating rapid thermal expansion due to the very high thermal conductivity of aluminium. However, immediately after reaching the peak value, the reaction force decreases drastically and becomes nearly zero at approximately 250-270 sec, indicating collapse or total loss of structural load-carrying capacity. Compared with steel and stainless steel, aluminium experiences severe degradation of strength and stiffness at a much lower temperature.

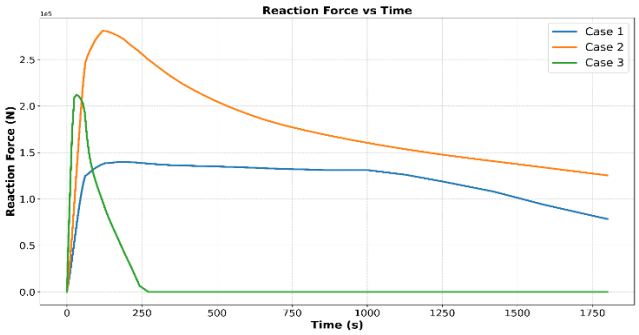


Fig. 10: Reaction force vs time graph for different cases

3.2.3 Protected Condition

The different thicknesses of magnesium oxide board (1-15 cm) are capable of reducing the fire temperature by 11.14% to 95.41%, respectively, under a 30-minute standard fire. Such a reduction in temperature is primarily attributed to the low thermal conductivity and high specific heat of magnesium oxide [19], thus making it a good thermal insulation material. The application of the required thickness of magnesium oxide board effectively mitigates the fire-induced instability in the building, as shown in Fig. 11, by restricting the stress and strain magnitudes within the permissible limits. A similar enhancement in the thermal performance of steel structural members after application of protective coatings was also reported by Džolev et al. [43] and Aghabozorgi et al. [44], who investigated intumescent coating and gypsum board as fire protection layers for steel members.

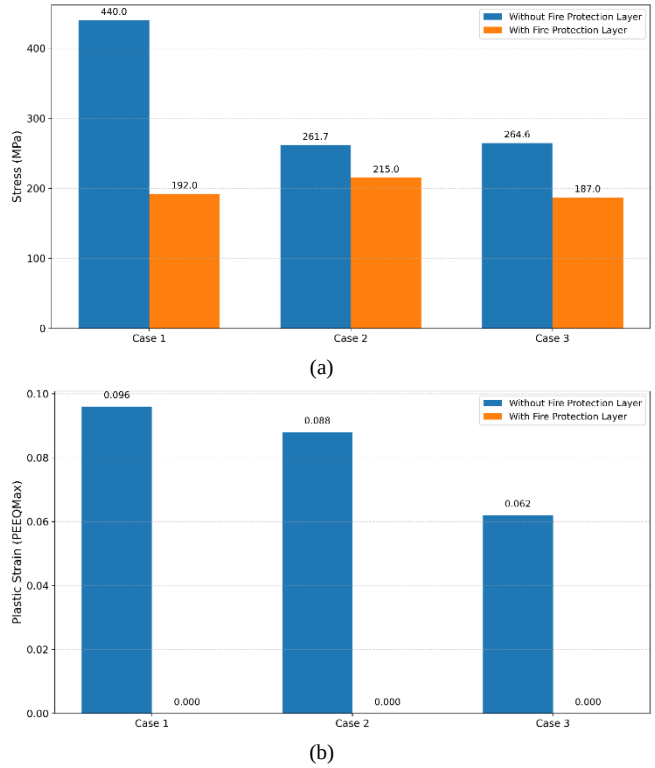


Fig. 11: Comparison of **(a)** stress and **(b)** strain in the building frame in unprotected and protected conditions under different cases

3.2.4 Initial Cost Analysis

An initial cost analysis of the structural steel, stainless steel, and aluminium frame has been carried out. The cost of a framed building is determined by many factors, including material cost, fire protection material and thickness, amount of material required, fabrication and erection costs. Conventional structural steel framing is generally the most economical solution due to it being widely available. Stainless steel is normally more costly to obtain; however, due to its corrosion resistance, it may benefit certain situations. Aluminium is generally less dense than steel, therefore reducing the weight of the structure; however, this depends on how large the members need to be, how they are fabricated, what the material costs are, and how the material performs under the design loads.

Fire protection also plays an important role in determining the most economic solution. The required material quantity and thickness determine the overall cost of fitting. From the numerical analysis it was found that the amount of fire protection material needed for the structural steel, stainless steel and aluminium was 10cm, 11cm and 8cm respectively. This shows that aluminium requires less fire protection than the other materials. However, this may vary depending on how much surface area needs to be protected. The cost will depend on how much surface area needs to be protected, what type of frame, the density of MgO boards, how they are fixed, how many layers there are, how they are sealed, and labour costs. The amount of fire protection will also depend on the required fire resistance rating and the temperature-dependent properties of each material.

Economic factors also need to be taken into account. The steel frame without any fire protection had the highest von Mises stress of 440MPa and an equivalent plastic strain of 0.096. The stainless steel frame had a maximum von Mises stress of 261.7MPa and an equivalent plastic strain of 0.088, and the aluminium frame had a maximum von Mises stress of 264.6MPa and an equivalent plastic strain of 0.062. Stainless steel also had the highest reaction forces throughout the simulation. The steel frame had a smoother variation of reaction force, and the aluminium frame showed a sudden large drop in reaction forces. It can be seen that the frames cannot be ordered simply based on the material cost or fire protection thickness. All aspects such as load-carrying capacity, deformation, stability, and the required fire resistance need to be considered.

Overall, it appears that structural steel may be a favourable option if the main priority is to keep the initial material costs low. Stainless steel may be favourable if durability and corrosion resistance can add value to the project. Aluminium could be favourable due to it having a lower weight, however the reaction forces dropped significantly due to the fire. This doesn't give a definite order, as this study didn't include verifiable market prices, detailed material takeoffs, fabrication and erection quotes, and life cycle costs. A quantitative analysis would need consistent data on the material cost for each of the structural materials, fire protection, fittings, maintenance, and replacement. It also needs to be verified that each of the options meets the same structural and fire resistance requirements. This analysis has been done to give an initial discussion on the cost performance of the materials.

4. Conclusions

The study presented a comparative thermo-mechanical assessment of steel, stainless steel, and aluminium frame buildings in a 30-minute standard fire. The effectiveness of the magnesium oxide board as a fire protection material was also evaluated. Based on the results obtained, the following conclusions can be drawn:

Fire exposure significantly causes an increase in stress and initiates plastic strain accumulation in all metallic-framed buildings considered. Steel showed the most severe fire-induced structural response in terms of stress and plastic strain. The least stress and plastic strain were exhibited by stainless steel and aluminium frames, respectively.

The critical temperature was found to vary with the metallic material used. The stainless steel frame showed the lowest critical temperature (60°C), the steel frame exhibited an intermediate critical temperature (71°C), while the aluminium frame shows the highest critical temperature (85°C), portraying that stress exceedance beyond the yield point and plastic strain accumulation in aluminium under fire requires more temperature compared to steel and stainless steel.

The reaction force analysis revealed distinct structural behaviour of all three metallic frames in fire. Stainless steel developed the highest reaction force throughout the fire duration. Steel exhibited intermediate behaviour, whereas aluminium showed rapid degradation in load capacity, indicating the most critical fire performance among all three cases considered.

Magnesium oxide board provided effective fire protection capabilities. Different thicknesses of 1-15 cm showed an efficiency of 11.14% to 95.41%, respectively, in reducing the peak fire temperature for 30 minutes. Based on the critical temperature criterion, the minimum board thickness required to maintain structural integrity for 30 minutes was found to be between 8-11 cm, depending on the case considered.

5. Scope of Future Work

The work can be extended further by considering various other parameters. Instead of the standard fire, external fire and hydrocarbon fire can be considered. Other protective coatings can be considered, such as composite, cement-based, and fibre-based. Cooling duration can be considered, and its effect can be determined. The beam-column connections can be modelled in detail, and their effect on the building's fire performance can be determined. The beams and columns with varying cross-sections can be considered. The effect of geometric irregularities in structural members can be included, and their effect on fire response can be determined.

6. Nomenclature

The following nomenclature has been used in this study:

S, Mises – Von Mises stress in steel.

PEEQMAX – Maximum equivalent plastic strain in steel

U_1 – Lateral displacement of the structure in the x direction

U_2 - Displacement of the beam in the y direction

U_3 – Lateral displacement of the structure in the z direction

References

[1] Amin, A., Tamal, S., Bari, A. K. M. F., Mazumder, M., & Hasan, M. A. (2022). Strengthening of fire-damaged reinforced beams by using ferro cement. Turkish Journal of Engineering, 6(3), 206-210. https://doi.org/10.31127/tuje.925199

[2] Liu, Y. J., & Li, H. N. (2004). Review and prospect of the study on behaviour of structures in fire conditions. *Journal of Disaster Prevention and Mitigation Engineering*, *24*(2), 219-225.

[3] Ahmed, A. D., & Güneyisi, E. (2022). Lateral response of double skin tubular column to steel beam composite frames. Turkish Journal of Engineering, 6(1), 16-25. https://doi.org/10.31127/tuje.749730

[4] Jelčić Rukavina, M., Skejić, D., Kralj, A., Ščapec, T., & Milovanović, B. (2022). Development of lightweight steel-framed construction systems for nearly-zero energy buildings. *Buildings*, *12*(7), 929. https://doi.org/10.3390/buildings12070929

[5] Czerwinski, F. (2020). Thermal stability of aluminium alloys. *Materials*, *13*(15), 3441. https://doi.org/10.3390/ma13153441

[6] Şahbaz, M. (2022). Comparison of experimental and numerical analysis of Quasi-Static punch shear test for stainless steel sheet material. Turkish Journal of Engineering, 6(4), 306-312. https://doi.org/10.31127/tuje.1002507

[7] You, X., Xing, Z., Jiang, S., Zhu, Y., Lin, Y., Qiu, H.,& Chen, Y. (2024). A review of research on aluminium alloy materials in structural engineering. *Developments in the built environment*, *17*, 100319. https://doi.org/10.1016/j.dibe.2023.100319

[8] Suman, S., & Samanta, A. (2020, March). Behaviour of Unrestrained Steel I-Section Beams in Case of Fire. In *Indian Structural Steel Conference* (pp. 737-748). Singapore: Springer Nature Singapore. https://doi.org/10.1007/978-981-19-9390-9_60

[9] Ibraheem, O. F., & Abdullah, H. A. (2022). Behaviour of Steel Beams Subjected to Bending and Shear Loading Under Localized Fire Conditions. *Tikrit Journal of Engineering Sciences*, *29*(3), 82-90. https://doi.org/10.25130/tjes.29.3.9

[10] Saleh, S. M., & Al-abboodi, İ. (2021). Strength and behaviour assessment of axially loaded concrete filled steel tubular stub columns. Turkish Journal of Engineering, 5(4), 154-164. https://doi.org/10.31127/tuje.686246

[11] İlgün, A., Zıa, A. J., Sancıoğlu, S., Soydoğan, H. F., Köklü, M. H., Arıbaş, S., & Bayram, B. (2023). Buckling performance of thin-walled filled steel columns. Turkish Journal of Engineering, 7(3), 172-179. https://doi.org/10.31127/tuje.1092975

[12] Quan, C., Murtaza, H., & Kucukler, M. (2023). Resistance and behaviour of carbon steel and stainless steel columns with axial and rotational end-restraints in fire. ce/papers, 6(3-4), 2214-2219. https://doi.org/10.1002/cepa.2508Digital Object Identifier (DOI)

[13] T. Hozjan, I. Planinc, M. Saje, S. Srpcic. (2008). Buckling of restrained steel columns due to fire conditions. Steel and Composite Structures, 8, 2, 159-178. https://doi.org/10.12989/scs.2008.8.2.159

[14] Taghipour Anvari, A., Mahamid, M., McNallan, M., & Eslami, M. (2019). Effectiveness of damaged fireproofing in structural steel members subjected to fire. *Journal of structural fire engineering*, *10*(1), 24-47. https://doi.org/10.1108/JSFE-11-2017-0044

[15] Aghabozorgi, P., Laím, L., & Santiago, A. (2025). Numerical and Design Analysis of Protected Steel Columns in Standard

Fire: P. Aghabozorgi et al. *Fire Technology*, *61*(5), 3093-3135. https://doi.org/10.1007/s10694-025-01716-y

[16] Bureau of Indian Standards. (1964). SP 6: (1), Handbook for structural engineers – Structural steel sections, New Delhi.

[17] Eurocode 3: Design of steel structures – Part 1 – 2: General rules – Structural fire design, EN-1993-1-2, 2005.

[18] Eurocode 9: Design of aluminium structures – Part 1 – 2: Structural fire design, EN-1999-1-2, 2007.

[19] Steau, E., & Mahendran, M. (2021). Elevated temperature thermal properties of fire protective boards and insulation materials for light steel frame systems. *Journal of Building Engineering*, *43*, 102571. https://doi.org/10.1016/j.jobe.2021.102571

[20] Bureau of Indian Standards. (1987). IS 875-Part 2, Code of Practice for Design Loads (Other Than Earthquake) For Buildings and Structures, New Delhi.

[21] The European Union. (2002). EN-1991-1-2, Eurocode 1: Actions on structures, in Part 1-2: Actions on structures exposed to fire.

[22] Lu, W., D'Mello, C., & Ayoub, A. (2020). Coupled thermomechanical damage modeling for structural steel in fire conditions. *Journal of* Structural Engineering, 146(7), 04020127. https://doi.org/10.1061/(ASCE)ST.1943-541X.0002652

[23] Zhu, G. M., Kang, Y. L., Chen, W., & Ma, G. T. (2008, April). 3D thermal mechanical coupled elasto-plastic finite element analysis in the whole rolling process of H-beam. In Materials Science Forum (Vol. 575, pp. 532-538). Trans Tech Publications Ltd. https://doi.org/10.4028/www.scientific.net/MSF.575-578.532

[24] BATOUNGUIDIO, S.A.M., & XUE, J. (2025). Finite Element Analysis of Steel Beams under Fire Exposure: The Impact of Geometric and Material Nonlinearity on Fire Resistance. International Journal of Research, 12(6). https://doi.org/10.5281/zenodo.15672233

[25] Ramesh, S., Choe, L., & Zhang, C. (2020). Experimental investigation of structural steel beams subjected to localized fire. Engineering structures, 218, 110844. https://doi.org/10.1016/j.engstruct.2020.110844

[26] Rubert, A., & Schaumann, P. (1986). Structural steel and plane frame assemblies under fire action. Fire Safety Journal, 10(3), 173-184. https://doi.org/10.1016/0379-7112(86)90014-7

[27] Bureau of Indian standards. (2007). IS 800:2007, General Construction in Steel-Code of Practice, New Delhi.

[28] Xing, Y., Wang, W., & Al-azzani, H. (2021). Assessment of thermal properties of various types of high-strength steels at elevated temperatures. Fire Safety Journal, 122, 103348.

[29] Pournaghshband, A., Afshan, S., & Theofanous, M. (2019, December). Elevated temperature performance of restrained stainless steel beams. In Structures (Vol. 22, pp. 278-290). Elsevierhttps://doi.org/10.1016/j.istruc.2019.08.015Get rights and content

[30] Rodrigues, J. C., Neves, I. C., & Valente, J. C. (2000). Experimental research on the critical temperature of compressed steel elements with restrained thermal elongation. Fire Safety Journal, 35(2), 77-98. https://doi.org/10.1016/S0379-7112(00)00018-7

[31] Allam, A., Nassif, A., & Nadjai, A. (2019). Behaviour of restrained steel beam at elevated temperature–parametric studies. Journal of Structural Fire Engineering, 10(3), 324-339. https://doi.org/10.1108/JSFE-11-2018-0036

[32] Wang, W., Zhang, L., Ge, Y., & Xu, L. (2018). Behaviour of restrained high strength steel columns at elevated temperature. Journal of Constructional Steel Research, 148, 251-264. https://doi.org/10.1016/j.jcsr.2018.05.022

[33] Lopes, N., Vila Real, P. M. M., Piloto, P. A. G., Mesquita, L. M. R., & Silva, L. S. (2006). Numerical modelling of the behaviour of a stainless steel portal frame subjected to fire.

[34] Maljaars, J., Soetens, F., & Snijder, H. H. (2010). Local buckling of fire-exposed aluminum members: New design model. Journal of structural engineering, 136(1), 66-75. https://doi.org/10.1061/(ASCE)ST.1943-541X.00000

[35] Milan, D., Torić, N., & Boko, I. (2022). Performance analysis of a simple aluminium structure in fire conditions. Advances in Civil and Architectural Engineering, 13(24), 12-22. https://doi.org/10.13167/2022.24.2

[36] Zanoni, A. L., Piloto, P. A., Mesquita, L., Rossetto, D. R., Lopes, N., & Vila Real, P. (2025). Fire resistance of stainless steel beams: different sections and grades. Journal of Structural Fire Engineering, 16(4), 566-593. https://doi.org/10.1108/JSFE-05-2025-0019

[37] Chen, T., Fan, S., Xu, Q., Xu, K., Luo, J., & Tang, Y. (2024). Research on mechanical properties of duplex stainless steel S22053 at elevated temperature and after fire. Thin-Walled Structures, 197, 111620. 10.1016/j.tws.2024.111620

[38] Choi, I. R., Chung, K. S., & Lee, H. (2017). Thermal and mechanical properties of structural steel SN400 at elevated temperatures. International Journal of Steel Structures, 17(3), 999-1007. https://doi.org/10.1007/s13296-017-9011-z

[39] Sabtu, M. A., Admi, A. E., Salleh, M. M., Osman, S. A., & Osman, S. A. (2024). Finite Element Analysis of Stress Distribution in AL6061 Frame Structures Under Varying Applied Loads. International Journal of Integrated Engineering, 16(2), 259-269.

[40] Petre, M., Dinu, C., Drăghici, N. C., & Andrei, V. (2020). Prediction of the residual stress after quenching of 6061 aluminium alloy plates by using mathematical modelling. In ITM Web of Conferences (Vol. 34, p. 02007). EDP Sciences.

[41] Cai, Y., Ho, H. W., Li, S., & Mensinger, M. (2025). Structural Metals after Exposure to High Temperatures: Residual Mechanical Properties and Predictions. steel research international, 96(7), 2400610. https://doi.org/10.1002/srin.202400610

[42] Zayniddinov, N., Volokhov, G., & Abdurasulov, S. (2025). Characterization and assessment of rolling stock structural durability under elevated operating temperatures. Vibroengineering Procedia, 60, 165-171.

[43] Džolev, I., Kekez-Baran, S., & Rašeta, A. (2025). Fire Resistance of Steel Beams with Intumescent Coating Exposed to Fire Using ANSYS and Machine Learning. Buildings, 15(13), 2334. https://doi.org/10.3390/buildings15132334

[44] Aghabozorgi, P., Laím, L., & Santiago, A. (2024). A Numerical Investigation On Fire Performance Of Industrial Steel Warehouses Protected With Gypsum-Based Boards. ce/papers, 7(1-2), 175-185. https://doi.org/10.1002/cepa.3034

This article is an open-access article distributed under the terms and conditions of the Creative Commons Attribution (CC-BY) license.